Charge densities and interionic potentials in simple metals: Nonlinear effects. II

L. Dagens
C.E.A., Centre d'Etudes de Limeil, BP No. 27, 94 Villeneuve St. Georges, France

Mark Rasolt
Department of Physics, University of Toronto, Toronto, Canada M5S 1A7

Roger Taylor*
Theoretical Physics Division, A.E.R.E. Harwell, Didcot, Oxon, England
(Received 24 June 1974)

We present nonlinear self-consistent calculations of the charge density induced by isolated Li^+, K^+, Mg^{++}, Al^{+++}, and Ca^{++} ions when placed in an electron gas of the appropriate metallic density. By comparison with linear-response theory we show that in the first four metals nonlinear effects in the response of the conduction electrons to the ionic perturbations play an important role in determining the charge density and the interionic potential. However as in the case of Na studied in the previous paper these nonlinear effects can be simulated by using a suitably adjusted model potential. The calculated phonon dispersion curves for Li, K, and Al agree very well with experiment. Nonlinear effects are also very likely to be important in Ca but further work is necessary before conclusions can be drawn.

I. INTRODUCTION

In the preceding paper,[1] referred to as I, the problem of calculating interionic potentials in simple metals is discussed. There it is pointed out that the solution of a closely related problem, that of the charge density induced by an isolated metallic ion in an electron gas, can be used as a guide to calculating a reliable interionic potential via standard pseudopotential theory. Briefly the procedure is as follows. First the charge density induced by an isolated ion, represented by a full ionic potential, in an electron gas is calculated. Next the equivalent linear-response solution, using a pseudopotential to represent the ion, is constructed. The pseudopotential parameters are then adjusted so that the linear-response charge density agrees very well with the nonlinear result for all r values outside the ionic core region. Finally the same pseudopotential parameters are used to calculate the interionic potential.

The need for invoking a procedure such as the above one arises from the fact that nonlinear effects turn out to be important in all the systems that we have studied. This fact is illustrated in the numerical example considered in I. The nonlinear charge density was taken from the Dagens[2] (referred to as II) calculation for an isolated Na^+ ion in an electron gas. A model potential was constructed to give the same phase shifts (by solving the Schrödinger equation) as the Na^+ ionic potential. This model potential, used in the linear-response approximation, not only gave rise to a charge density differing somewhat from the nonlinear calculation but also to phonon frequencies which were generally about 10% higher than the experimental ones. However, by following the procedure described above the phonon frequencies turned out to agree very well with experiment. Hence it was concluded that (i) nonlinear effects are important even in Na and (ii) these effects could be taken into account by using a model potential adjusted to generate, via linear-response theory, the correct nonlinear charge density.

In this paper we extend the calculations of I and II to a number of other simple metal systems, i.e., Li^+, K^+, Mg^{++}, Al^{+++}, and Ca^{++}, with two objectives in mind. These are (i) to present nonlinear self-consistent calculations of the charge density induced by each of these ions when placed in an electron gas of the appropriate metallic density and (ii) to use these calculations in conjunction with the equivalent linear-response results in order to analyze and correct for nonlinear effects in the response of electrons to ionic perturbations. The nonlinear charge densities were obtained by solving the Hartree-Fock equations employing the usual Gaspar-Kohn-Sham (GKS) $\rho^{1/3}$ exchange approximation as well as the Hartree approximation. The procedure was essentially the same as given in II, some details of which are given in Sec. II of this paper. The metallic charge density is then given quite accurately by a superposition of these isolated ion densities.[2-4]

For the linear-response calculations we used in each case an energy-independent nonlocal model potential of similar form to that introduced by Heine and Abarenkov.[5] With the exception of Ca an energy-independent model potential is a good approximation in the materials we are considering, but for most of them nonlocal effects are known

to be important.[6] In our case we found it essential to use nonlocal model potentials for two reasons. First, in attempting to elucidate precisely the effect of nonlinearity it is necessary to construct a model potential which is formally equivalent to the ionic potential used for the nonlinear calculations. This can be achieved by requiring the model potential to give the same phase shifts over a wide range of r and, with the possible exception of K, a nonlocal model potential is required.[6] In Al, e.g., the use of a local model potential, which best reproduced the full ionic phase shifts, gave fair agreement with the nonlinear charge density. The error, however, was very much reduced when a nonlocal one (giving the *same* phase shifts as the full ionic potential for a wide range of r) was used instead. Secondly, we found in practice that when adjusting the model-potential parameters to include nonlinear effects, an accurate main peak and the long-range oscillations in the charge density could only be obtained, in all cases, with a nonlocal model potential. This is particularly true in Li where a local "fit" to the charge density gives errors of $\gtrsim 50\%$ in the amplitude of the long-range oscillations.[7] When one observes that even the near-neighbor region of an interionic potential is strongly influenced by the charge-density oscillations it becomes increasingly clear that nonlocality must be taken into account.

In Sec. II we summarize the theoretical basis for the calculations which are presented in Sec. III. There we show that for K, Al, Li, and Mg nonlinear effects are significant but can be corrected for by the procedure of adjusting the model potential to the charge density just as in I. In each case the effect of nonlinearity is to shift the main peak of the charge density towards the origin and to lower the calculated phonon frequencies. The results and conclusions are summarized in Sec. IV.

II. THEORETICAL BASIS

In this section we outline briefly the theoretical basis behind the calculations which are presented in Sec. III. First we describe the neutral atom model for the charge distribution in a metal and also the nonlinear self-consistent (NLSC) procedure used to calculate it. Then we describe the procedure used to generate the linear-response charge density which is to be compared with the self-consistent result.

A. Neutral atom model

The self-consistent valence density $\rho_{\rm val}(\vec{r})$ of a simple metal can be calculated accurately by means of the neutral atom model.[2-4] This theory assumes that $\rho_{\rm val}(\vec{r})$ can be written with little error as a sum over the metal ions of rigid neutral atom densities $n(\vec{r}-\vec{R})$ centered on the various ion positions $\vec{R}$.[8] The important fact is that $n(r)$ is structure independent and depends only upon the mean valence density ρ_0, the ionic potential $V_{\rm ion}$, and the assumed valence-valence exchange and correlation potential $\mu_{\rm xc}$. The neutral atom method allows a direct calculation of $n(r)$ by solving an auxiliary impurity problem, which amounts to the self-consistent calculation of the *nonlinear* screening of an isolated neutral impurity potential, embedded in the neutralized electron gas which represents the zero-order metal valence density. This impurity potential V_0 is simply related to the ionic potential $V_{\rm ion}$. Its expression is

$$V_0 = V_{\rm ion} + (e^2/r)\,\nu(r)\ , \tag{1}$$

where $V_{\rm ion}$ is the one-particle ionic potential to be described later, and $\nu(r)$ a spherical charge density which represents intuitively that part of the unperturbed valence density ρ_0 which neutralizes the corresponding ion. The form of $\nu(r)$ is rather arbitrary. It must be chosen such that the sum of $\nu(|\vec{r}-\vec{R}|)$ over the atomic sites $\vec{R}$ approximates the unperturbed valence density ρ_0 as closely as possible, for the physically significant structures. Ball[3] uses a uniform auxiliary screening density ($\mu=\rho_0$ inside the ionic Wigner-Seitz sphere and zero outside). We use in the present work the trapezoidal form described by Dagens[4] which leads to significantly smaller $\rho_0-\sum_{\rm ions}\nu$ for most metal structures.

The calculation of $n(r)$ proceeds as follows. V_0 is embedded in the neutralized electron gas, of uniform density ρ_0, and the self-consistent displaced charge $n'(r)$ is calculated numerically as described in II. This auxiliary neutral density n' differs from $n(r)$ by the quantity $n''(r)$ which represents the effect of the nonphysical compensating charge $\nu(r)$. More precisely, $\sum_{\rm ions} n'$ represents the charge density displaced by the potential $\sum_{\rm ions} V_0$ when all multiple scattering terms are neglected. This potential includes the unphysical contribution $\Delta v_0=(e^2/r)\,(\sum\nu-\rho_0)$ which induces a spurious displaced density which we write as $\rho_0-\sum n''$ [see II, Eq. (11)] and which must be subtracted from $\rho_0+\sum n'$. Now, Δv_0 is very small, and we neglect again all the multiple-scattering terms involving Δv_0 and any V_0. $\rho_0-\sum n''$ is then given by the standard linear-response theory, and $n''(r)$ is found to be the Fourier transform of

$$n''(q) = -\,[1/\epsilon(q)]\nu(q)\ .$$

$n''(r)$ is obtained by numerical Fourier transform and added to $n'(r)$ to make the rigid neutral atom density $n(r)=n'(r)+n''(r)$ [II, Eqs. (11), (12)].

The main assumption of the neutral atom theory is that V_0 is a weak scatterer, such that all multiple-scattering terms involving at least two differ-

ent scatterers are indeed negligible. It is not necessary to assume that V_{ion} is small, and an exact (one-particle) ionic potential may be used. $n(r)$ includes thus all nonlinear contributions which originate from repeated scattering on a given ion, but not, of course, the nonlinearity associated to the scattering over two or more distinct ions.

Three kinds of ionic potentials have been considered in the present work, in order to appreciate how much the screening charge $n(r)$ is sensitive to the choice of a specific ionic potential. The first one is the Hartree-Fock-Slater GKS ionic potential previously used[2] with the $\rho^{1/3}$ Gaspar-Kohn-Sham exchange potential. The second one is a semiempirical potential fitted to observed atomic term values. Such potentials are available for Li^+,[9] Na^+,[10] K^+,[11] Mg^{++},[6] Ca^{++},[6] and Al^{+++}.[6] This potential is local and is expected to simulate accurately the Hartree-Fock plus correlation ionic potential. The last potential which has been used is the nonlocal Hartree-Fock potential (HF ionic potential $V_{\text{ion}}^{\text{HF}}$). $V_{\text{ion}}^{\text{HF}}$ has been taken equal to the ionic part of the HF self-consistent potential of the corresponding isolated atom. The neutral atom computing program previously used,[2,4] has been modified in order to deal with such a nonlocal potential[12] and applied to Li, Na, and Al.

We comment here briefly the results of these calculations. We have compared, for a few metals (Li, Na, K, and Al) the neutral atom densities obtained for the three ionic potentials (GKS, empirical, and HF), using the same valence-valence GKS exchange potential. We have found that the computed neutral atom density is very little dependent upon the specific ionic potential. More precisely, the corresponding variation $4\pi r^2|\Delta n|$ of the radial neutral atom density $4\pi r^2 n(r)$ has been always found to be less than 1.5% of the largest maximum of $4\pi r^2 n$. Such a difference is of little significance in the present context, and only the results relative to the empirical ionic potentials will be presented in latter parts of this work.

We discuss now the valence-valence indirect interaction potential. It is taken as a simple function $\mu_{xc}(\rho_{\text{val}})$ of the valence density. The Hartree or random-phase-approximation (RPA) screening is obtained when $\mu_{xc} \equiv 0$. The $\rho^{1/3}$ Gaspar-Kohn-Sham approximation is used for the exchange part. The Nozières-Pines (NP) formula

$$\mu_c(\rho) = \mu_c(\rho_0) - 0.00517 \ln \rho(\vec{r})/\rho_0$$

has been used for the correlation part in a few calculations. We have found that the effect of this correlation potential upon the density $n(r)$ is rather small. The corresponding correction $4\pi r^2 \Delta n$ for Li is found to be less in magnitude than about 2% of the maximum of $4\pi r^2 n$, for example. The correlation part will thus be omitted in the following and only RPA and GKS results will be compared with the corresponding linear screening densities.

B. Linear response

To calculate the linear-response results we proceed in the same manner as in I. To make a meaningful comparison with the NLSC results it is necessary to construct a pseudopotential which is formally equivalent to the ionic potential used to generate them. In each case we have used a model potential of the form

$$V_p = \sum_l \left(A_l \Theta(R_l - r) - (Ze^2/r)\Theta(r - R_l)\right)\hat{P}_l ,$$

where $\Theta(x)$ is the usual step function and $\hat{P}_l$ is the angular momentum projection operator. For l values greater than or equal to a value l_0, we have taken $A_l = A_{l_0}$ and $R_l = R_{l_0}$. In Li $l_0 = 1$, and in all other cases $l_0 = 2$. The parameters were then adjusted to reproduce the phase shifts of the ionic potential for $r > R_L$ (the largest of the values of R_0) at the Fermi energy. The fit obtained was in each case similar to that obtained for Na in I. The phase shifts were also calculated at other energies where for all materials except Ca they agreed very well with the ionic phase shifts. Thus, as is well known (e.g., Ref. 6) an energy-independent model potential was found to be satisfactory for Li, K, Mg, and Al but not for Ca. The parameters for these model potentials, referred to as M1, are given in Table I.

The NLSC charge densities were calculated using both the Hartree approximation and the GKS exchange approximation. In the limit of linear response the corresponding screening functions are, respectively,[1] the RPA or Hartree screening and the exchange screening given by

$$\Pi_x(q) = \frac{\Pi_0(q)}{1 - \pi e^2 \Pi_0(q)/k_F^2} .$$

$\Pi_0(q)$ is the RPA result. These then are the screening functions that were used to generate in

TABLE I. Model-potential parameters used for the calculations in this paper. The $M1$ parameters have been adjusted to reproduce the ionic-potential phase shifts and the $M2$ parameters to reproduce the NLSC charge densities. The values of A_l are in Ry and R_l in a.u.

		A_0	R_0	A_1	R_1	A_2	R_2
Li	$M1$	−0.454	2.07	−1.435	2.07	−1.435	2.07
	$M2$	−0.70	2.38	−1.32	2.38	−1.32	2.38
K	$M1$	−0.377	3.002	−0.377	3.32	−1.17	3.32
	$M2$	−0.32	2.65	−0.32	3.08	−1.80	3.08
Mg	$M1$	−1.235	1.82	−1.235	1.66	−3.80	1.66
	$M2$	−1.235	1.72	−1.235	1.50	−3.80	1.50
Al	$M1$	−2.22	1.515	−2.22	1.38	−6.70	1.38
	$M2$	−2.22	1.45	−2.22	1.31	−6.70	1.31
Ca	$M1$	−1.00	2.577	−1.00	2.69	−3.085	2.69

each case the appropriate linear-response charge density. The formula for this quantity, describing the screening of a nonlocal pseudopotential, is given by Eq. (39) of I.

It is a simple matter (see I) to extend the theory for the charge density to the problem of calculating phonon dispersion curves in the solid assuming the validity of the neutral atom model discussed earlier in this section. Essentially this is nothing more than the problem of calculating the energy of a system corresponding to the charge density already computed. Hence a theory giving rise to an accurate charge density should also give rise to accurate phonon dispersion curves within the limits of the neutral atom model. Conversely, errors in the charge density will be reflected in these quantities. Thus by comparing the computed phonon dispersion curves with experiment we are able to assess the significance of any errors in the linear-response charge densities. With this in mind we have computed both phonon dispersion curves and interionic potentials using Eq. (43) of I for the energy–wave-number characteristic. In this case, however, since we are comparing with experimental quantities we have used the Geldart and Taylor[13] approximation to the electron gas screening function since this quantity contains correlations as well as exchange and goes beyond the first gradient term.

The only numerical example considered in I was Na. There it was found that although the linear-response charge density agreed quite well with the NLSC result, the errors arising from the omission of the nonlinear terms were significant. However by adjusting the model potential parameters so that the linear-response charge density coincided with the NLSC density for $r \gtrsim R_L$ it was found that the corresponding phonon dispersion curves, which previously were in error by about 10%, agreed very well with experiment. Thus it was concluded that the effect of nonlinearity could be simulated by a suitably adjusted linear term. Hence for some of the calculations described in Sec. III we have made similar adjustments to the model potential parameters and we shall refer to these by the symbol $M2$. The values chosen for the $M2$ parameters are also listed in Table I.

III. RESULTS AND DISCUSSION

Before discussing each metal separately we make some general comments about the charge densities presented in Figs. 1, 4, 7, 10, and 12. In each case the NLSC result, both with and without exchange, contains one or more oscillations at small r. These are due to the need for the wave function to be orthogonal to the tightly bound ionic core electrons. These oscillations are of course not present in the model potential results due to the absence of core electrons.[1] The oscillations at large r are the well-known Friedel oscillations which are a manifestation of the well-defined Fermi surface. These oscillations are also present in the interionic potentials shown in Figs. 3, 6, 8 and 11. It is clear from these figures that even the near-neighbor region is strongly influenced by the Friedel oscillations, and hence it is important to obtain the right amplitude for the oscillations in order to produce a reliable interionic potential.

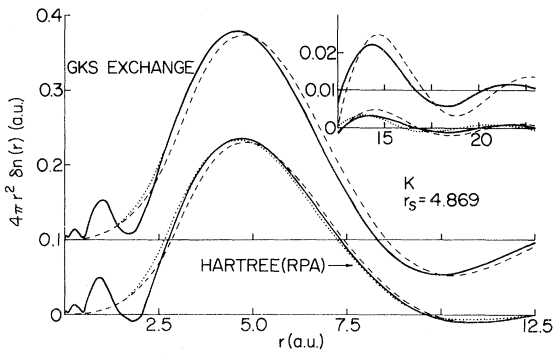

FIG. 1. Charge densities induced by an isolated K^+ ion in an electron gas. For clarity the GKS exchange results are displaced upwards by 0.1 a.u. (0.01 a.u. in the inset) relative to the Hartree results; solid line, nonlinear self-consistent calculations; dashed, linear-response calculation with model potential $M1$; dotted, linear-response calculation with model potential $M2$.

Potassium

In Fig. 1 are displayed the charge densities calculated using the Hartree and GKS exchange approximations. The NLSC results are indicated by a solid line and the corresponding linear-response results (model potential $M1$) by a dashed line. The agreement between the two is quite good, being similar to that obtained in I for Na. The calculations for model potential $M2$ are indicated by a dotted line. Several points are worth commenting on. In Na[1] and Li, Al, and Mg (see below) the $l = 2$ parameter of the model potential has a negligible effect. In K, however, its effect is larger and probably reflects a small effect of the low-lying unfilled d states. Although these can introduce only a slight energy dependence in the $l = 2$ parameter of K, they have a much greater effect in Ca, where they lie just above the Fermi level, giving rise to model-potential parameters which are strongly energy dependent.[6] Also (see Fig. 1) adjustment for nonlinear effects, done so that the exchange density is best reproduced, results in some error in the Hartree density and again could reflect the slight effect of energy dependence in the model potential. Since the exchange density more closely approximates the

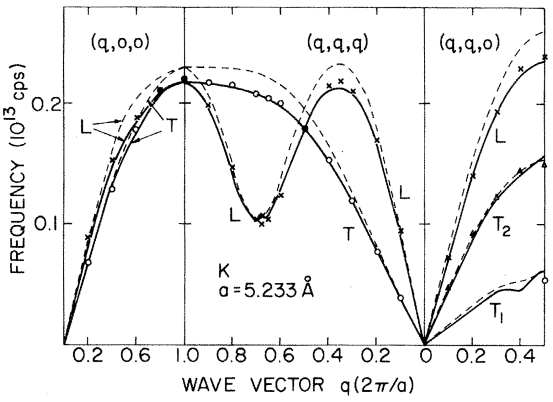

FIG. 2. Phonon dispersion curves at 9 °K for K. The experimental points which are taken from Cowley *et al.* (Ref. 14) are indicated by × for longitudinal branches and o and Δ for transverse branches. Dashed line, $M1$ model potential; solid, $M2$ model potential.

true metallic density, the appropriate pair potential was constructed via that density.

An examination of the calculated phonon dispersion curves in Fig. 2 shows that, just as in the case of sodium, by adjusting the model-potential parameters to correct for the nonlinear terms in the charge density, the errors in the phonon frequencies are almost completely removed.

The interionic potentials resulting from the $M1$ and $M2$ model potentials are shown in Fig. 3, where it can be seen that as in the sodium case the effect of the nonlinear corrections is to deepen the first well and to shift the phase of the oscillations towards the origin.

Aluminium

The charge densities calculated using both the Hartree and the GKS exchange approximations are displayed in Fig. 4. Here the agreement between

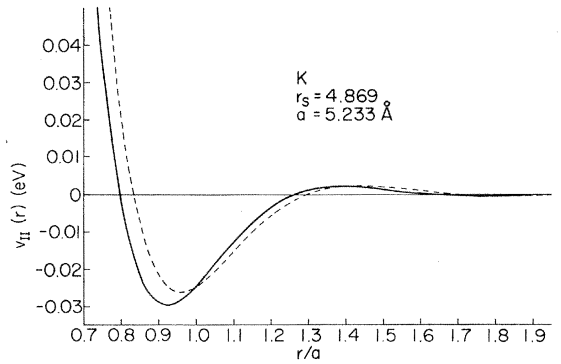

FIG. 3. Interionic potential for K calculated using the $M1$ (dashed line) and $M2$ (solid line) model potentials.

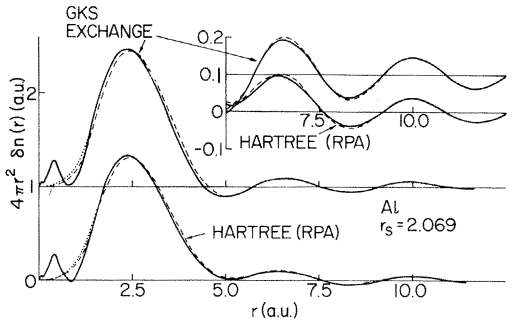

FIG. 4. Charge densities induced by an isolated Al^{+++} ion in an electron gas. For clarity the GKS exchange results are displaced upwards by 1.0 a.u. (0.1 a.u. in the inset) relative to the Hartree results. The notation is the same as for Fig. 1.

both the NLSC and the linear-response ($M1$) results is remarkably good. It appears therefore that increasing the number of valence electrons does not decrease the validity of linear-response theory.

Nevertheless the small differences between the two charge densities are still significant, as can be seen by examining the phonon dispersion curves shown in Fig. 5. The frequencies calculated using the $M1$ model potential are typically about 10% too high. And just as in Na and K the $M2$ model potential, which in this case fits both the NLSC exchange and Hartree results, generates very good agreement with the experimental phonon frequencies. At first sight it might seem surprising that such a small difference in the charge densities should be reflected in such a large discrepancy in the phonon curves. However Vosko *et al.*[16] have pointed out that in Al the screening effect of the electron gas cancels the pure Coulomb repulsion between the ions to a much greater degree than

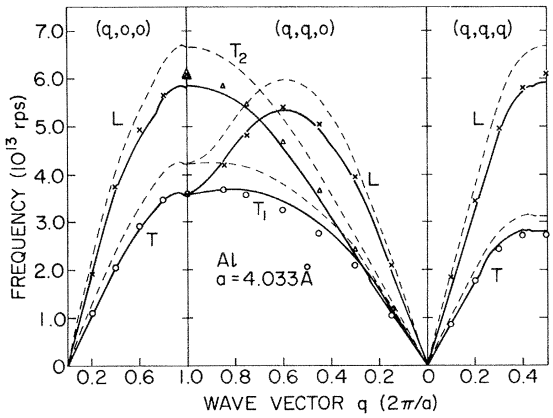

FIG. 5. Phonon dispersion curves at 90 °K for Al. The experimental points are taken from Stedman and Nilsson (Ref. 15) and the notation is the same as that for Fig. 2.

in the alkali metals. Hence the calculated phonon frequencies of Al will be far more sensitive to small errors in the electron-ion interaction and we are forced to conclude that also in this system nonlinear effects are important. However, as in Na and K, they can be simulated to a large degree by a suitably adjusted linear-response term.

It should be pointed out that Al, having a Fermi surface which is strongly distorted by the zone boundary, will show extra structure in the phonon dispersion arising from the presence of Kohn anomalies,[17] their positions and strength being dictated by the true distorted Fermi surface. (Experimentally the Kohn anomalies have been measured very accurately in Al.)[18] These obviously are nonlinear effects not corrected for by our approach, hence, our Kohn anomalies do not appear at the same points as the experimental ones and a comparison is not very meaningful. However, since our interest is in constructing interionic potentials (to be used, e.g., in liquid metals, etc.) these effects are of no relevance to this work.

The interionic potentials resulting from the $M1$ and $M2$ model potentials are compared in Fig. 6 where it can be seen that the principal effect of nonlinearity is in the first-neighbor region. The unusual appearance of the interionic potential in this region, i.e., large and positive, is due to the choice of electron gas screening, not to the choice of model potential.[19]

Lithium

The calculated charge densities are displayed in Fig. 7. The NLSC results computed using the GKS exchange approximation differ somewhat from the calculations reported in II. This is due to the fact that the trapezoidal form of the neutralizing spherical charge density $\nu(r)$ [Eq. (1)] was used rather than the Gaussian form. This leads to a

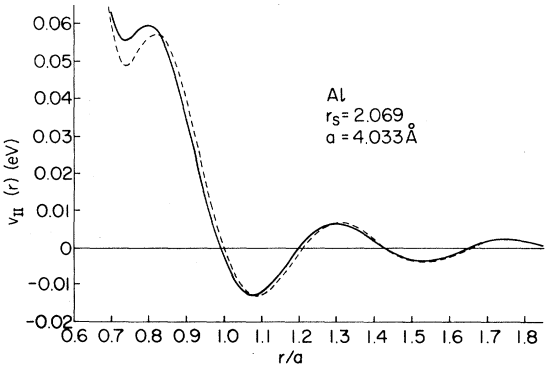

FIG. 6. Interionic potential for Al calculated using the $M1$ (dashed line) and $M2$ (solid line) model potentials.

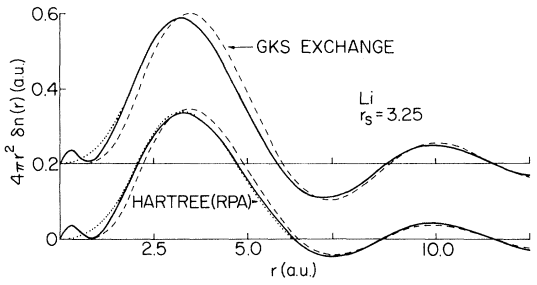

FIG. 7. Charge densities induced by an isolated Li^+ ion in an electron gas. For clarity the GKS exchange results are displaced upwards by 0.2 a.u. relative to the Hartree results. The notation is the same as for Fig. 1.

significantly smaller potential Δv_0. In principle, this should not affect the calculations, but due to the fact that Δv_0 is treated via linear-response theory, the use of the trapezoidal form of $\nu(r)$ leads to the more accurate results that are shown in Fig. 7.

When considering Li from the pseudopotential point of view it is useful to note that although a weak pseudopotential can be constructed to reproduce the s-phase shifts correctly, this is not the case for the p-phase shifts. This is due to the absence of p-electrons in the core, which means that the p-components of the conduction electrons see the full ionic potential and the equivalent pseudopotential must therefore be a strong potential. Thus Li is not only extremely nonlocal but should also be more nonlinear than the other systems we have considered. This certainly seems to be the case when we compare the $M1$ linear-response charge densities with NLSC results in Fig. 7. There is somewhat greater discrepancy here than in the other systems. This is reflected in greater errors (15%–20%) in the phonon dispersion curves shown in Fig. 8. Following our procedure of constructing model potential $M2$ to give the same charge density as the NLSC calculation (in this case exchange only as in K) we see that there is considerable improvement in the phonon dispersion curves but there still remain errors of order 5%.

There are quite a few possible reasons for the remaining errors in the phonon frequencies. It is likely that in view of the fact that Li is strongly nonlinear, we are not justified in expecting that all the nonlinear effects can be simulated by a linear term. Hence it could be that because Li is such a strong scatterer, three- and four-body forces play a larger role in the lattice dynamics and that our use of the neutral atom model is not as well justified. Another possible effect is that of anharmonicity. Li is a very light ion and there may well be important anharmonic effects even at liquid-nitrogen temperature. If the trends are

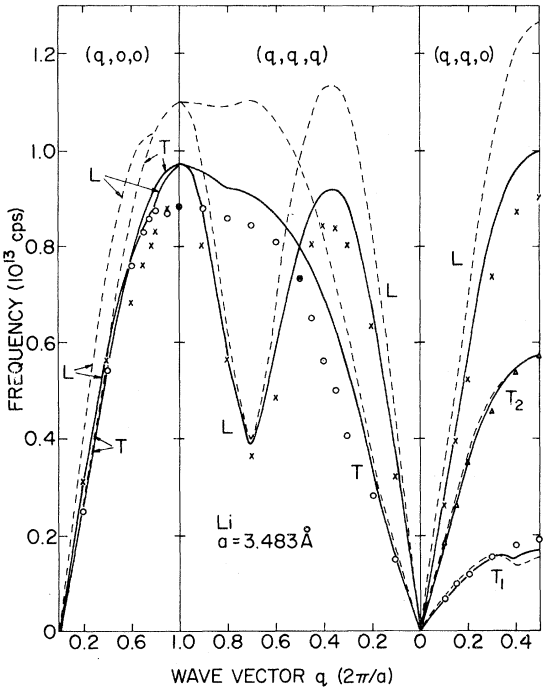

FIG. 8. Phonon dispersion curves at 90 °K for Li. The experimental points are taken from Smith *et al.* (Ref. 20) and the notation is the same as for Fig. 2.

the same as in ^{21}Na and ^{10}K then the phonon modes will tend to soften, thus reducing the discrepancy between theory and experiment. Clearly these are points which would be worth investigating further.

A very interesting feature of the experimental Li phonon curves is the crossover which takes place between the [100] L and T branches about halfway across the zone. This feature is reproduced by the $M2$ calculations and can be identified with the presence of a Kohn anomaly at approximately $q = 0.8\ (2\pi/a)$ in the [100] L branch. This

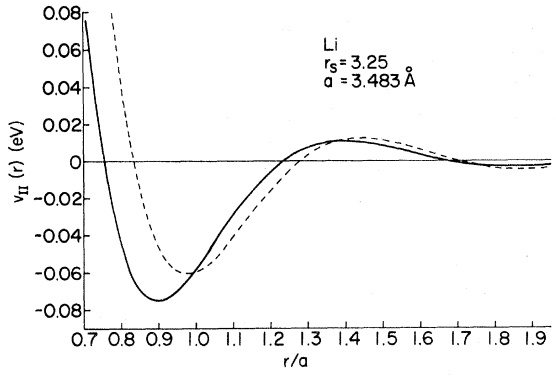

FIG. 9. Interionic potential for Li calculated using the $M1$ (dashed line) and $M2$ (solid line) model potentials.

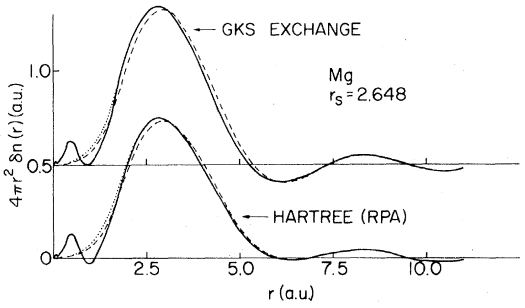

FIG. 10. Charge densities induced by an isolated Mg^{++} ion in an electron gas. For clarity the GKS exchange results are displaced upwards by 0.5 a.u. relative to the Hartree results. The notation is the same as for Fig. 1.

has the effect of depressing the longitudinal branch in this region to a point where it lies well below the transverse branch. The amplitude of the anomaly is dependent on the energy–wave-number characteristic $F(q)$ [Eq. (43) of I] at $q = 2k_F$, which in turn depends on the degree of nonlocality in the model potential. Due to the high degree of nonlocality in Li there exists a large amplitude for the Kohn anomaly and hence the large effect on the phonon curves. The large amplitude for the long-range oscillations in the charge density is a manifestation of the same effect. Kohn anomalies occur in both Na and K at the same place, but due to the fact that nonlocality is not nearly so important an effect in either of these metals, the anomalies are very weak and are not observed experimentally.

The interionic potentials calculated with both the $M1$ and $M2$ model potentials are shown in Fig. 9. Here the effect of nonlinearity is the same as in Na and K. The initial well is deepened, and the phase of the oscillations is moved towards the origin. The depth of the well is more than a factor of 2 greater than in Na and K, and the oscillations are much stronger. This is again a manifestation of the strong nonlocality in Li.

Magnesium

The charge densities calculated using both the Hartree and the GKS exchange approximations are illustrated in Fig. 10. The agreement between the NLSC results and the linear-response ($M1$) results is nearly as good as that obtained for Al. Hence it seems likely that nonlinear effects will be of similar importance to those in Al. In this case, as with Al, the $M2$ model potential gives a good fit to both the Hartree and the GKS charge density.

We have not calculated phonon frequencies for Mg but in Fig. 11 we show the effect of nonlinearity on the interionic potential by comparing results

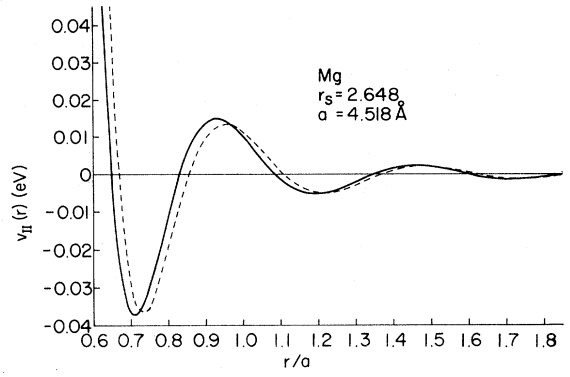

FIG. 11. Interionic potential for Mg calculated using the $M1$ (dashed line) and $M2$ (solid line) model potentials. Note that the parameter a in this case has been chosen for convenience to be the cube edge of a fcc lattice of the same density as the true hcp lattice.

calculated using the $M1$ and $M2$ model potentials. As in the other materials the values of r are given in terms of a parameter a, which requires some explanation since Mg metal forms a hexagonal close-packed structure. For reasons of computational convenience a was chosen to be the cube edge of a face-centered cubic lattice with the same density as Mg metal. Hence the first-neighbor distance is at $r = 0.707a$. Thus, the Mg interionic potential is quite conventional looking with the first well positioned in the near-neighbor region. The effect of nonlinearity is to shift the phase of the potential oscillations towards small r so that the bottom of this well is right at the first-neighbor site.

Calcium

The calcium charge densities calculated with both Hartree and GKS exchange approximations are displayed in Fig. 12. It is interesting to note that the amplitude of the NLSC long-range oscillations is considerably larger than in Mg, suggesting that Ca is quite a strong scatterer and that nonlinear effects could be very important. Although the $M1$ linear-response calculations seem to agree quite well in the region of the main peak, it is clear that the amplitude and phase of the long-range oscillations are very poor. Also in contrast to the other materials, the main peak of $M1$ charge density is shifted, relative to the NLSC result, towards the origin rather than the other way around.

A very important feature of Ca that has been ignored in the linear-response calculation is the presence of unfilled d states situated just above the Fermi level. It is well known (see, e.g., Ref. 6) that when such a situation occurs the $l = 2$ component of the pseudopotential becomes strongly energy dependent. Hence our use of an energy-independent model potential is invalid. The Ca phase shifts, are then well represented only near the Fermi energy by the $M1$ model potential. Therefore before any conclusions can be drawn about the effect of nonlinearity in Ca the energy dependence of the model-potential parameters must be taken into account. It seems likely that the poor results for the $M1$ long-range oscillations as well as the unusual positioning of the main charge-density peak are largely due to the omission of energy-dependence. It would be interesting to investigate this point further.

We have not attempted to fit an energy-independent model to the Ca charge density nor have we calculated an interionic potential since clearly these results would have little or no physical significance.

IV. SUMMARY AND CONCLUSIONS

In this paper we have presented nonlinear self-consistent calculations of the charge density induced by isolated Li^+, K^+, Mg^{++}, Al^{+++}, and Ca^{++} ions placed in an electron gas of the same density as the corresponding metal. The metallic density can then be generated, within the framework of the neutral atom model, by a linear superposition of the isolated ion densities. We have also calculated the charge densities generated by linear-response theory using in each case a model potential ($M1$) which is formally equivalent to the full ionic potential used in the nonlinear calculation. Generally speaking, although the agreement between the two calculations seemed to be quite good, the differences or nonlinear effects turned out to be important. By adjusting the model potential parameters ($M2$) to fit the NLSC charge densities we found that in K, Al, and Li the calculated phonon frequencies gave much better agreement with experiment. Just as for Na, reported in I, the phonon frequencies generated by the $M1$ model potential were too high whereas the $M2$ frequencies gave very good agreement with experiment in K

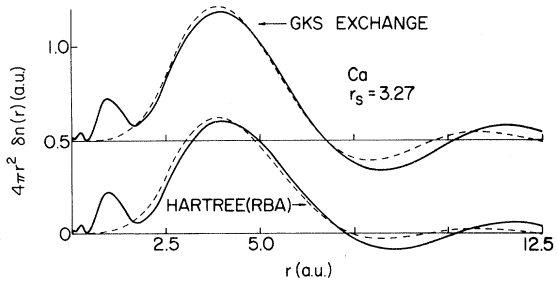

FIG. 12. Charge densities induced by an isolated Ca^{++} ion in an electron gas. For clarity the GKS exchange results are displaced upwards by 0.5 a.u. relative to the Hartree results. The notation is the same as for Fig. 1.

and Al and considerably improved agreement in Li. The fact that the density plays such a central role in cohesive energy calculations and the success of the above procedure in the calculation of phonon frequencies strongly suggests that the resulting interionic potentials should be considerably more reliable.

We have not calculated the Mg phonon dispersion curves but we have no reason to doubt that the same effects will occur there too. Hence, the $M2$ interionic potential should be just as reliable as the others.

Due to the fact that the energy dependence of a model potential for Ca is a very important effect we have not proceeded further than the energy-independent linear-response calculations illustrated in Fig. 12. It seems very likely that nonlinearities will be of similar importance in this system, but before any definite conclusions can be drawn the energy dependence of the model potential must be taken into account.

Finally we comment that due to space restrictions we are not able to publish listings of the interionic potentials. But these including Na, tabulated for more than one density, are available as a Harwell report.[22]

ACKNOWLEDGMENTS

One of us (R. T.) would like to thank the Theoretical Physics Division, A. E. R. E. Harwell for their hospitality during a one-year visit.

*Permanent address: Physics Division, National Research Council, Ottawa, Canada K1A OR6.

[1]M. Rasolt and R. Taylor, preceding paper, Phys. Rev. B, 11, 2717 (1975).
[2]L. Dagens, J. Phys. C 5, 2333 (1972).
[3]M. A. Ball, J. Phys. C 2, 1248 (1969).
[4]L. Dagens, J. Phys. (Paris) 34, 879 (1973).
[5]V. Heine and I. V. Abarenkov, Philos. Mag. 9, 451 (1964).
[6]M. Rasolt and R. Taylor, J. Phys. F 2, 270 (1972); 3, 67 (1973).
[7]M. Rasolt and R. Taylor, J. Phys. F 3, 1678 (1973).
[8]J. M. Ziman, Adv. Phys. 13, 89 (1964).
[9]F. Seitz, Phys. Rev. 47, 400 (1935), corrected by W. Kohn and N. Rostoker, *ibid.* 94, 111 (1954).
[10]W. K. Prokofjew, Z. Phys. 58, 255 (1929); corrected by E. P. Wigner and F. Seitz, Phys. Rev. 43, 804 (1933).
[11]M. S. Duesbery, R. Taylor and H. R. Glyde, Phys. Rev. B 8, 1372 (1973).
[12]L. Dagens and L. Degove (unpublished).
[13]D. J. W. Geldart and R. Taylor, Can. J. Phys. 48, 167 (1970).
[14]R. A. Cowley, A. D. B. Woods, and G. Dolling, Phys. Rev. 150, 487 (1966).
[15]R. Stedman and G. Nilsson, Phys. Rev. 145, 492 (1966).
[16]S. H. Vosko, R. Taylor, and G. H. Keech, Can. J. Phys. 43, 1187 (1965).
[17]W. Kohn, Phys. Rev. Lett. 2, 393 (1959).
[18]R. Stedman and G. Nilsson, Phys. Rev. Lett. 15, 634 (1965); J. W. Weymouth and R. Stedman, Phys. Rev. B 2, 4743 (1970).
[19]M. S. Duesbery and R. Taylor, Phys. Rev. B 7, 2870 (1973).
[20]H. G. Smith, G. Dolling, R. M. Nicklow, P. R. Vijayaraghavan, and M. K. Wilkinson, *Neutron Inelastic Scattering* (International Atomic Energy Authority, Vienna, 1968), Vol. 1, p. 149.
[21]H. R. Glyde and R. Taylor, Phys. Rev. B 4, 1206 (1972).
[22]Contact The Secretary, Radiation Damage Group, Theoretical Physics Division, Building 8.9, A. E. R. E. Harwell, Didcot, Oxon., England for the A. E. R. E. Harwell Theoretical Physics Report No. T. P. 579 (unpublished).